RESEARCH ARTICLE OPEN ACCESS

Brain Characteristics in Patients With Myelin Oligodendrocyte Glycoprotein Antibody-Associated Disorder by 7.0 Tesla MRI

Lei Su[1,2,3] | Joseph Kuchling[4,5] | Chenyang Gao[1,2,3] | Thoralf Niendorf[4,6] | Carsten Finke[4,5] | Zhe Zhang[1,2] | Ai Guo[1,2] | Jing Jing[1,2] | De-Cai Tian[1,2] | Yu-Jing Li[3] | Mengting Zhang[1,2] | Xiaoyu Shi[1,2] | Xinyao Liu[1,2] | Huabing Wang[1,2] | Yaou Liu[7] | Claudia Chien[4] | Michael Levy[8] | Yunyun Duan[7] | Friedemann Paul[4,5] | Fu-Dong Shi[1,2,3]

[1]Tiantan Neuroimaging Center of Excellence, China National Clinical Research Center for Neurological Diseases, Beijing Tiantan Hospital, Capital Medical University, Beijing, China | [2]Department of Neurology, Beijing Tiantan Hospital, Capital Medical University, Beijing, China | [3]Department of Neurology, Tianjin Medical University General Hospital, Tianjin, China | [4]Experimental and Clinical Research Center, Max Delbrueck Center for Molecular Medicine, Charité Universitätsmedizin Berlin, Berlin, Germany | [5]Department of Neurology, Charité Universitätsmedizin Berlin, Berlin, Germany | [6]Berlin Ultrahigh Field Facility, Max Delbrueck Center for Molecular Medicine in the Helmholtz Association, Berlin, Germany | [7]Department of Radiology, Beijing Tiantan Hospital, Capital Medical University, Beijing, China | [8]Department of Neurology, Massachusetts General Hospital and Harvard Medical School, Boston, Massachusetts, USA

Correspondence: Friedemann Paul (friedemann.paul@charite.de) | Fu-Dong Shi (fshi@tmu.edu.cn)

ABSTRACT

Background: Myelin oligodendrocyte glycoprotein antibody-associated disease (MOGAD) can radiographically mimic multiple sclerosis (MS) and neuromyelitis optica spectrum disorder (NMOSD). The disease hallmarks cortical lesion, central vein sign (CVS) and paramagnetic rim lesions identified in MS have not yet been comprehensively investigated in MOGAD.

Methods: We have characterized 45 patients with MOGAD using 7.0 Tesla (7 T) MRI at two academic research hospitals in China and Germany. 7 T MRI, laboratory, and clinical data were collected. The classification of cortical lesions, proportion of CVS, and the phase shifts of lesions on susceptibility weighted imaging were analyzed.

Results: Of the 45 patients enrolled with MOGAD, 282 lesions were identified. We further detected 31 (11%) cortical lesions including leukocortical, intracortical, and subpial types, of which intracortical lesions (16/31, 52%) were frequently involved. CVS was identified in 53 (19%) lesions of 21 (47%) patients, 154 (55%) lesions showed multiple veins sign (MVS) in 30 (67%) patients. The number (4.3 ± 6.0 vs. 1.5 ± 2.1, $p = 0.0049$) and percentage (52% vs. 18%, $p < 0.0001$) of MVS lesions for each MOGAD patient were higher than those of CVS. Eight patients (18%) had 39 (14%) lesions of hypointense signal with paramagnetic phase shifts on SWI, showing nodular phase changes and irregular borders in appearance.

Conclusions: In our observational MOGAD cohort, all three types of cortical lesions were recognized, with intracortical lesions being the most common. The number and proportion of lesions with MVS were higher than those with CVS. Lesions with paramagnetic phase changes were rare and non-rim-like in appearance. These findings provide a better understanding of the underlying pathology of MOGAD and will help in the differentiation of MOGAD from other demyelinating disorders.

Lei Su, Joseph Kuchling, and Chenyang Gao contributed equally to this work.

---

1 | Introduction

Myelin oligodendrocyte glycoprotein antibody-associated disease (MOGAD) is a recently recognized and independent disease entity. MOGAD is typically associated with acute disseminated encephalomyelitis, optic neuritis, or transverse myelitis. The presence of high titers ($\geq$ 1:100) of MOG immunoglobulin G in serum (MOG-IgG) is unique to MOGAD [1, 2]. In cases where the MOG-IgG titer is low (< 1:100) or not available, the diagnosis of MOGAD depends on additional clinical and MRI features.

The MRI characteristics that help differentiate MOGAD from MS and NMOSD in the optic nerves and spinal cords are longitudinally extensive lesions, perineural optic sheath enhancement, and central lesions or H sign in spinal cord lesions. With regard to brain lesions, supportive MRI features of MOGAD are subjective and are generally focused on the presence of multiple ill-defined T2-hyperintense lesions in the supratentorial or infratentorial regions and leptomeningeal enhancement with and without cerebral cortical lesions [3–6]. Perivenous inflammation, myelin loss, and MOG-laden macrophages were observed in pathological studies of MOGAD [7, 8], which lead to the hypothesis that patients with MOGAD would exhibit lesions with central vein sign (CVS) [9] and paramagnetic rims (PRL) [10] in advanced MR imaging. However, these features have not yet been studied in MOGAD using 7 T MRI, which provides enhanced spatial resolution and magnetic susceptibility to detect anatomical and pathological features in greater detail compared to clinical field strengths at 1.5 or 3 T [11, 12].

With this background, we enrolled patients with MOGAD to characterize MRI features of brain lesions, including lesion distribution, classification of cortical lesions, proportion of CVS, and phase shifts of lesions at 7 T.

2 | Materials and Methods

2.1 | Participants

From January 2018 to January 2024, imaging, laboratory, and clinical data of patients with MOGAD were collected from two academic research hospitals: Beijing Tiantan hospital (Beijing, China) and Charité Universitätsmedizin Berlin (Berlin, Germany). All patients were re-evaluated according to the latest proposed diagnostic criteria of the International MOGAD Panel [1]. Inclusion criteria were as follows: (1) age between 14 and 65; (2) at least one acute clinical demyelinating episode of the central nervous system (myelitis, optic neuritis, or cerebral attack) lasting at least 24 h; (3) serum or cerebrospinal fluid (CSF) MOG-IgG positivity in cell-based assay (CBA); (4) serum AQP4-IgG negativity; and (5) the exclusion of a better diagnosis including MS. Exclusion criteria: (1) incomplete clinical assessment; (2) poor MRI image quality; (3) history of other neurological or neuropsychological conditions (e.g., stroke or dementia); (4) contraindications for ultra-high-field MRI, such as implanted metallic devices, pregnancy, etc. Patients with serum MOG-IgG titers of less than 1:100 or positive CSF MOG-IgG only, who presented with one of the core clinical attack types, were required

to have at least one supporting clinical or MRI feature and after exclusion of other diagnoses including MS, were diagnosed with MOGAD [1]. All patients completed 7 T MRI examinations. Clinical data such as sex, age, disease duration, expanded disability status scale (EDSS) score, and each clinical episode were collected in detail. According to the time from last attack to 7 T scan, MOGAD patients were stratified into an acute phase group (no more than 28 days) and a non-acute phase group (more than 28 days). To better illustrate characteristics of patients with cortical lesions and/or CVS, clinical and paraclinical data of these patients with focus on MOGAD and MS diagnostic criteria are also summarized (Table S3). A flow chart of enrollment is presented in Figure 1.

Ethical approval for this study was obtained from the Ethical Committee of Beijing Tiantan Hospital (KY2021-150-01) and Charité Universitätsmedizin Berlin (EA1/222/17), and written informed consent was obtained from all participating individuals according to the Declaration of Helsinki.

2.2 | MRI Acquisition

MRI studies were performed on two 7 T MRI Siemens scanners (Siemens Healthcare, Erlangen, Germany). The scanning protocol consisted of 3D magnetization-prepared rapid acquisition gradient echoes (T1-MPRAGE) imaging, including whole brain coverage, fluid-attenuated inversion recovery (FLAIR) imaging, susceptibility weighted imaging (SWI), and multi-echo T2*-weighted spoiled gradient echo imaging. FLuid And White matter Suppression (FLAWS) based on the magnetization-prepared with two rapid gradient echoes (MP2RAGE) sequence (FLAWS-MP2RAGE) was adopted for better detecting lesions at Beijing Tiantan Hospital. The FLAWS-MP2RAGE sequence produces three sets of images, including two inversion times (INV1 and INV2) and a corrected image (UNI). The sequence parameters are listed in Table S1.

Eligibility criteria
- Individuals with demyelinating episode of CNS
- Age: between 14 to 65
- serum or CSF MOG-IgG positive
- serum AQP4-IgG negative
- the exclusion of a better diagnosis including MS

Assessed for eligibility
from January 2018 to January 2024
n=50

Excluded for incompatibility
with 2023 MOGAD diagnostic criteria
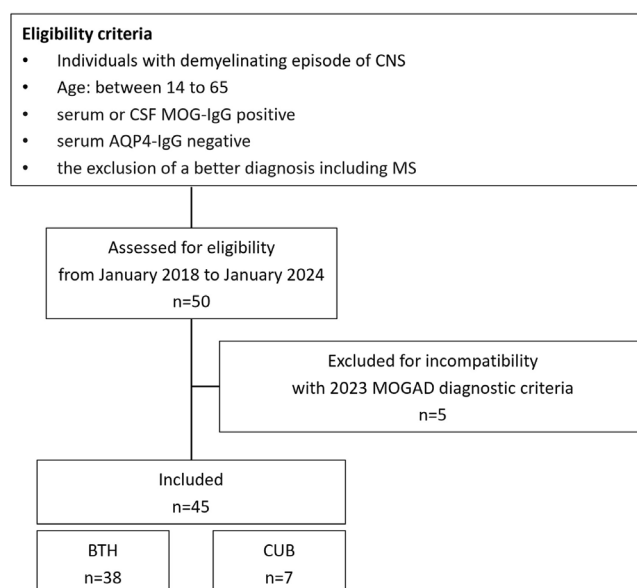n=5

Included
n=45

BTH
n=38

CUB
n=7

FIGURE 1 | Flow chart for enrollment. BTH, Beijing Tiantan Hospital; CUB, Charité Universitätsmedizin Berlin.

2.3 | Image Analysis

2.3.1 | Lesion Identification and Labeling

Lesion identification and segmentation was performed by three experienced readers from neurology (C.G. and L.S.) and radiology (Z.Z.). A lesion was defined as a T2-FLAIR hyperintense signal alteration extending over at least 2 mm [13], and imaging information from T2-FLAIR combined with T1-MPRAGE and FLAWS-MP2RAGE was used to determine the respective location of each lesion, especially regarding cortical lesions. All lesions were segmented using 3D Slicer software (https://www.slicer.org/) [14]. Lesions were classified into white matter lesions, cortical lesions, deep gray matter lesions, brainstem lesions, and cerebellar lesions. White matter lesions were classified into juxtacortical lesions, periventricular lesions, corpus callosum lesions, and other white matter lesions (Figure S1). Confluent lesions were excluded from this study.

2.3.2 | Types of Cortical Lesions

Cortical abnormal signals that are linear or tubular or less than 1.0 mm in width were excluded to eliminate cortical vessels. Classification of three types of cortical lesions was performed according to previously published criteria [15, 16]: Leukocortical (traversing white and gray matter), intracortical (located exclusively within cortex), and subpial (more widespread areas of cortical signal abnormality, arising at the subpial surface, usually in deep sulci and/or traversing multiple sulci or gyri).

2.3.3 | CVS and Phase Shifts

For all identified lesions, CVS was evaluated on T2* weighted MRI. Lesional phase changes were examined on SWI. CVS was defined according to the 2016 consensus statement of the North American Imaging Multiple Sclerosis (NAIMS) Cooperative [9]. The central vein was identified on images in at least two perpendicular planes as a thin hypointense line or small hypointense dot with a small apparent diameter (<2 mm), located in the center of the lesion and passing through it at least partially or completely. Lesions were excluded from CVS assessment if they fused with other lesions, appeared to contain multiple visible veins, or were poorly visible. We also identified the lesions containing multiple veins, each of which can be seen in at least two perpendicular planes, and we labeled this particular feature that lesions contained multiple veins as multiple veins sign (MVS) (Figure 3). Phase shifts of the lesions were divided into four categories [17]: (1) lesions with paramagnetic phase changes at the edge of the lesions, (2) lesions with paramagnetic phase changes in the center of the lesions that are nodular in appearance, (3) lesions without any intralesional phase changes, and (4) lesions with diamagnetic phase changes (Figure S2).

MRI image analysis at each step above, including lesion identification, cortical lesion classification, CVS identification, and phase shifts analysis, was based on the consensus of two independent raters (C.G. and L.S.) and another senior neuroimaging expert (Z.Z.), who reviewed the cases of disagreement.

2.3.4 | Statistical Analysis

All analyses were performed using IBM SPSS Statistics (version 26; IBM, Armonk, NY). Categorical data were expressed as percentages. Continuous data are expressed as means and standard deviations (SD), and ranked data were expressed as medians and IQR. Groups were compared descriptively using chi-squared tests for categorical measures, Mann–Whitney *U* test for nonparametric data, and independent *t*-test for parametric data in both the groups. The ICC was calculated as a two-way mixed test of single measures using the consistency model to evaluate the agreement between the two raters. A *p*-value below 0.05 was considered statistically significant.

3 | Results

3.1 | Clinical Characteristics

A total of 45 patients with MOGAD were finally enrolled in this study, with a male-to-female ratio of 1.05:1 and a median EDSS score of 2 (range 0–8.5). The 45 MOGAD patients had a total of 154 clinical events, of which 11 patients were in the acute phase, which was defined as ≤28 days since the last attack. Optic neuritis (59/154, 38%) was the most common symptom, followed by myelitis (30/154, 20%) and cerebral monofocal and polyfocal CNS deficits associated with demyelinating lesions (27/154, 18%). Others included brainstem and cerebellar deficits (20/154, 13%), cerebral cortical encephalitis (17/154, 11%) and acute disseminated encephalomyelitis (ADEM) (1/154, 1%). Thirteen MOGAD patients had a total of 17 cerebral cortical encephalitis attacks often with seizures, of which five patients were in the acute phase. Three of these patients had extensive FLAIR hyperintense cortical lesions and were considered as patients presenting with FLAIR-hyperintense lesions in anti-MOG-associated encephalitis with seizures (FLAMES). The clinical characteristics between the acute phase group and non-acute phase group were not significantly different. The detailed demographic and clinical characteristics are shown in Table 1 and Table S2. A detailed summary of clinical and brain MRI characteristics in the Chinese center and the German center is shown in the Tables S4 and S5. Patients acquired in the Chinese center had significantly shorter time from the last attack to MRI, a shorter disease duration, a lower optic neuritis frequency, a higher frequency in cerebral attack, and a higher frequency in brainstem and cerebellar deficits.

3.2 | Interrater Reliability

Raters worked independently, blinded to clinical data. They had a good interrater agreement. The intraclass correlation (ICC) was 0.91 for brain lesion count, the number of leukocortical lesions (ICC = 0.90), the number of intracortical lesions (ICC = 0.89), the number of subpial lesions (ICC = 0.86), the number of lesions with a central vein (ICC = 0.93) and multiple

TABLE 1 | Demographic and clinical characteristics in MOGAD cases within the acute phase and within the non-acute phase.

MOGAD	Total	MOGAD patients within the acute phase[a]	MOGAD patients in the non-acute phase[b]	*p*
No.	45	11	34	
Female/male	1:1.05	1.2:1.00	1:1.13	0.666
Age, years, mean ± SD (range)	33.80 ± 12.09 (15–59)	33.27 ± 12.80 (15–57)	33.97 ± 12.05 (17–59)	0.870
Ethnicity				
Asian, *n*/total (%)	38/45 (84.4)	11/11 (100)	27/34 (79.4)	0.168
Caucasian, *n*/total (%)	7/45 (15.6)	0/11 (0)	7/34 (20.6)	0.168
Disease duration, months, median (IQR)	21 (2–39)	5 (2–40)	23.5 (1.75–47.25)	0.441
Time from last attack to MRI, months, median (IQR)	2 (1–18)	0.6 (0.43–0.83)	5.5 (1.45–22.73)	< 0.001
Number of attacks, median (IQR)	2 (1–3)	2 (1–3)	2 (1–4)	0.765
No. of patients on disease modifying therapy	19/45 (9 rituximab; 6 MMF; 2 AZA; 1 MTX; 1 tocilizumab)	3/11 (2 rituximab; 1 MMF)	16/34 (7 rituximab; 5 MMF; 2 AZA; 1 MTX; 1 tocilizumab)	
EDSS score, median (IQR)	2 (1–3.5)	3.5 (1–4.5)	2 (0.75–3)	0.152
Core clinical demyelinating event				
ON, *n*/total (%)	59/154 (38.3)	13/38 (34.2)	46/116 (39.7)	0.571
Myelitis, *n*/total (%)	30/154 (19.5)	6/38 (15.8)	24/116 (20.7)	0.639
ADEM, *n*/total (%)	1/154 (0.6)	0/38 (0)	1/116 (0.9)	> 0.999
Cerebral monofocal or polyfocal deficits, *n*/total (%)	27/154 (17.5)	8/38 (21.1)	19/116 (16.4)	0.623
Brainstem and cerebellar deficits, *n*/total (%)	20/154 (13.0)	4/38 (10.5)	16/116 (13.8)	0.783
Cerebral cortical encephalitis often with seizures, *n*/total (%)	17/154 (11.0)	7/38 (18.4)	10/116 (8.6)	0.132

Abbreviations: ADEM, acute disseminated encephalomyelitis; AZA, azathioprine; BTH, Beijing Tiantan Hospital; CUB, Charité Universitätsmedizin Berlin; MMF, mycophenolate mofetil; MTX, methotrexate; ON, optic neuritis.

[a]Acute phase was defined as the time between the last attack and the 7 T MRI scan of 28 days or less.

[b]Non-acute phase was defined as the time between the last attack and the 7 T MRI scan of more than 28 days.

veins (ICC = 0.93), the number of lesions with paramagnetic phase change and hypointense signal on SWI (ICC = 0.96), and the number of lesions with isointense signals on SWI without phase changes (ICC = 0.84).

3.3 | Lesion Distribution of MOGAD on 7T MRI

Based on FLAIR, 3D-T1 MPRAGE, and FLAWS-MP2RAGE, 282 lesions were identified in 36 MOGAD patients. Nine patients showed no brain lesions. There were 228 white matter lesions (228/282, 81%), 31 cortical lesions (31/282, 11%), 6 deep gray matter lesions (6/282, 2%), 16 brainstem lesions (16/282, 6%), and one cerebellum lesion (1/282, 0.4%). White matter lesions included 37 juxtacortical lesions (37/282, 13%), 10 periventricular lesions (10/282, 4%), six corpus callosum lesions (6/282, 2%), and 175 other white matter lesions (175/282, 62%) (Table 2).

3.4 | Characteristics of Cortical Lesions in MOGAD

A total of 31 cortical lesions were observed in 12 of the 45 patients with MOGAD, which were classified according to 3D-T1 MPRAGE and FLAWS-MP2RAGE, and T2-FLAIR (Figure 2). Thirty-two percent (10/31) were leukocortical lesions spanning the gray–white matter, 52% (16/31) intracortical lesions, and 16% (5/31) subpial cortical lesions. Seven of the twelve individuals with cortical lesions did not have clinical demyelinating events of cerebral cortical encephalitis (Table 2).

TABLE 2 | Brain MRI characteristics in MOGAD cases within the acute phase and within the non-acute phase.

MOGAD	Total	MOGAD patients within acute phase[a]	MOGAD patients in non-acute phase[b]	p
	n = 45	n = 11	n = 34	
Brain lesions				
Presence of brain lesions, No./total (%)	36/45 (80.0)	10/11 (90.9)	26/34 (76.5)	0.298
Total number of lesions, n (median, IQR)	282 (2, 1–6.25)	43 (3, 2–7)	239 (2, 0.75–8.25)	0.523
Cortical, n/total (%)	31/282 (11.0)	7/43 (16.3)	24/239 (10.0)	0.706
WM, n/total (%)	228/282 (80.9)	28/43 (65.1)	200/239 (83.7)	0.630
Juxtacortical, n/total (%)	37/282 (13.1)	3/43 (7.0)	34/239 (14.2)	0.969
Periventricular, n/total (%)	10/282 (3.5)	4/43 (9.3)	6/239 (2.5)	0.327
Corpus callosum, n/total (%)	6/282 (2.1)	0/43 (0)	6/239 (2.5)	0.575
Other WM, n/total (%)	175/282 (62.1)	21/43 (48.8)	154/239 (64.4)	0.845
Deep GM, n/total (%)	6/282 (2.1)	3/43 (7.0)	3/239 (1.3)	0.367
Brainstem, n/total (%)	16/282 (5.7)	5/43 (11.6)	11/239 (4.6)	0.907
Cerebellum, n/total (%)	1/282 (0.4)	0/43 (0)	1/239 (0.4)	0.886
Cortical lesions, n (median, IQR)	31 (0, 0–1)	7 (0, 0–0)	24 (0, 0–1)	0.635
Leukocortical, n/total (%)	10/31 (32.3)	1/7 (14.3)	9/24 (37.5)	0.990
Intracortical, n/total (%)	16/31 (51.6)	5/7 (71.4)	11/24 (45.8)	0.845
Subpial, n/total (%)	5/31 (16.1)	1/7 (14.3)	4/24 (16.7)	> 0.999
CVS				
Patients with CVS+ lesions, No./total (%)	21/45 (46.7)	7/11 (63.6)	14/34 (41.2)	0.194
Lesions with CVS, n/total (%)	53/282 (18.8)	7/43 (16.3)	46/239 (19.2)	0.647
Cortical, n/total (%)	3/31 (9.7)	0/7 (0)	3/24 (12.5)	0.325
WM, n/total (%)	47/228 (20.6)	6/28 (21.4)	41/200 (20.5)	0.909
Juxtacortical, n/total (%)	2/37 (5.4)	0/3 (0)	2/34 (5.9)	0.666
Periventricular, n/total (%)	0/10 (0)	0/4 (0)	0/6 (0)	/
Corpus callosum, n/total (%)	0/6 (0)	0/0 (0)	0/6 (0)	/
Other WM, n/total (%)	45/175 (25.7)	6/21 (28.6)	39/154 (25.3)	0.750
Deep GM, n/total (%)	0/6 (0)	0/3 (0)	0/3 (0)	/
Brainstem, n/total (%)	3/16 (18.8)	1/5 (20.0)	2/11 (18.2)	0.931
Cerebellum, n/total (%)	0/1 (0)	0/0 (0)	0/1 (0)	/
Average CVS+ rate (per individual patient) (%)	18	22	16	0.433
Number of patients met the 40% CVS+ proportion threshold, No./total (%)	7/45 (15.6)	3/11 (27.3)	4/34 (11.8)	0.217
Number of patients met 3 CVS+ lesions, No./total (%)	7/45 (15.6)	0/11 (0)	7/34 (20.6)	0.168

(Continues)

TABLE 2 | (Continued)

MOGAD	Total	MOGAD patients within acute phase[a]	MOGAD patients in non-acute phase[b]	p
	n = 45	n = 11	n = 34	
MVS				
Patients with MVS+ lesions, No./total (%)	30/45 (66.7)	8/11 (72.7)	22/34 (64.7)	0.726
Lesions with MVS, n/total (%)	154/282 (54.6)	22/43 (51.2)	132/239 (55.2)	0.623
Cortical, n/total (%)	5/31 (16.1)	1/7 (14.3)	4/24 (16.7)	0.880
WM, n/total (%)	137/228 (60.1)	16/28 (57.1)	121/200 (60.5)	0.837
Juxtacortical, n/total (%)	31/37 (83.8)	3/3 (100)	28/34 (82.4)	0.427
Periventricular, n/total (%)	8/10 (80.0)	2/4 (50.0)	6/6 (100)	0.053
Corpus callosum, n/total (%)	1/6 (16.7)	0/0 (0)	1/6 (16.7)	/
Other WM, n/total (%)	97/175 (55.4)	11/21 (52.4)	86/154 (55.8)	0.818
Deep GM, n/total (%)	4/6 (66.7)	2/3 (66.7)	2/3 (66.7)	> 0.999
Brainstem, n/total (%)	8/16 (50.0)	3/5 (60.0)	5/11 (45.5)	> 0.999
Cerebellum, n/total (%)	0/1 (0)	0/0 (0)	0/1 (0)	/
Average MVS rate (per individual patient) (%)	52	52	52	0.794
Phase shifts of lesions				
Paramagnetic phase shift, n/total (%)	39/282 (13.8)	2/43 (4.7)	37/239 (15.4)	0.058
Nodular, n/total (%)	29/282 (10.3)	0/43 (0)	29/239 (12.1)	0.016
Irregular, n/total (%)	10/282 (3.5)	2/43 (4.7)	8/239 (3.3)	0.670
No phase shift	243/282 (86.2)	41/43 (95.3)	202/239 (84.5)	0.758

Abbreviations: BTH, Beijing Tiantan Hospital; CUB, Charité Universitätsmedizin Berlin; CVS, central vein sign; GM, gray matter; MVS, multiple veins sign; WM, whiter matter.

[a]Acute phase was defined as the time between the last attack and the 7T MRI scan of 28 days or less.

[b]Non-acute phase was defined as the time between the last attack and the 7T MRI scan of more than 28 days.

3.5 | Central Vein Sign in MOGAD

A total of 21 patients (21/45, 47%) had CVS positive lesions, and 53 (53/282, 19%) of all lesions (median: 1; range: 0–8) showed a central vein. The average CVS positive rate per individual patient was 18%, and seven patients (7/45, 16%) had more than 40% CVS positive lesions. Only seven patients (7/45, 16%) had more than three brain lesions with CVS. The CVS was present in 47 white matter lesions (47/228, 21%), three cortical lesions (3/31, 10%), three brainstem lesions (3/16, 19%), 0 cerebellum lesion (0/1, 0%), and 0 deep gray matter lesion (0/6, 0%). The white matter lesions included 2 juxtacortical lesions (2/37, 5%), 0 periventricular lesion (0/10, 0%), 0 corpus callosum lesion (0/6, 0%), and 45 other white matter lesions (45/175, 26%). We also found 30 (30/45, 67%) patients exhibiting MVS positive lesions and 154 (154/282, 55%) lesions (median: 2; range: 0–25) showed MVS. The average MVS rate per individual patient was 52%. The MVS was present in 137 white matter lesions (137/228, 60%), five cortical lesions (5/31, 16%), eight brainstem lesions (8/16, 50%), 0 cerebellum lesion (0/1, 0%), and four deep gray matter lesions (4/6, 67%). The white matter lesions included 31 juxtacortical lesions (31/37, 84%), eight periventricular lesions (8/10, 80%), one corpus callosum lesion (1/6, 17%), and 97 other white matter lesions (97/175, 55%) (Table 2). The number (4.3 ± 6.0 vs. 1.5 ± 2.1, $p = 0.0049$) and percentage (52% vs. 18%, $p < 0.0001$) of MVS lesions for each patient were significantly higher than those of CVS lesions in MOGAD (Figure 3). The volume of MVS positive lesions (median, $35.9\,mm^3$; IQR, 18.9–$118.8\,mm^3$) was higher than the volume of CVS positive lesions (median, $22.1\,mm^3$; IQR, 10.3–$37.6\,mm^3$) ($p < 0.001$). Representative CVS and MVS lesions of MOGAD are shown in Figure 3.

3.6 | Phase Shifts of Lesions on SWI

Thirty-nine (39/282, 14%) hypointense lesions with paramagnetic phase on SWI were identified in eight patients with MOGAD, including 29 nodular lesions and 10 irregular border lesions in appearance (Figure 4). There was no significant difference in MOG-IgG titer, disease duration, number of attacks, and EDSS score between these eight patients with paramagnetic phase lesions and patients without lesions with phase shifts. The percentage of nodular paramagnetic lesions was higher in patients in the non-acute phase compared with patients in
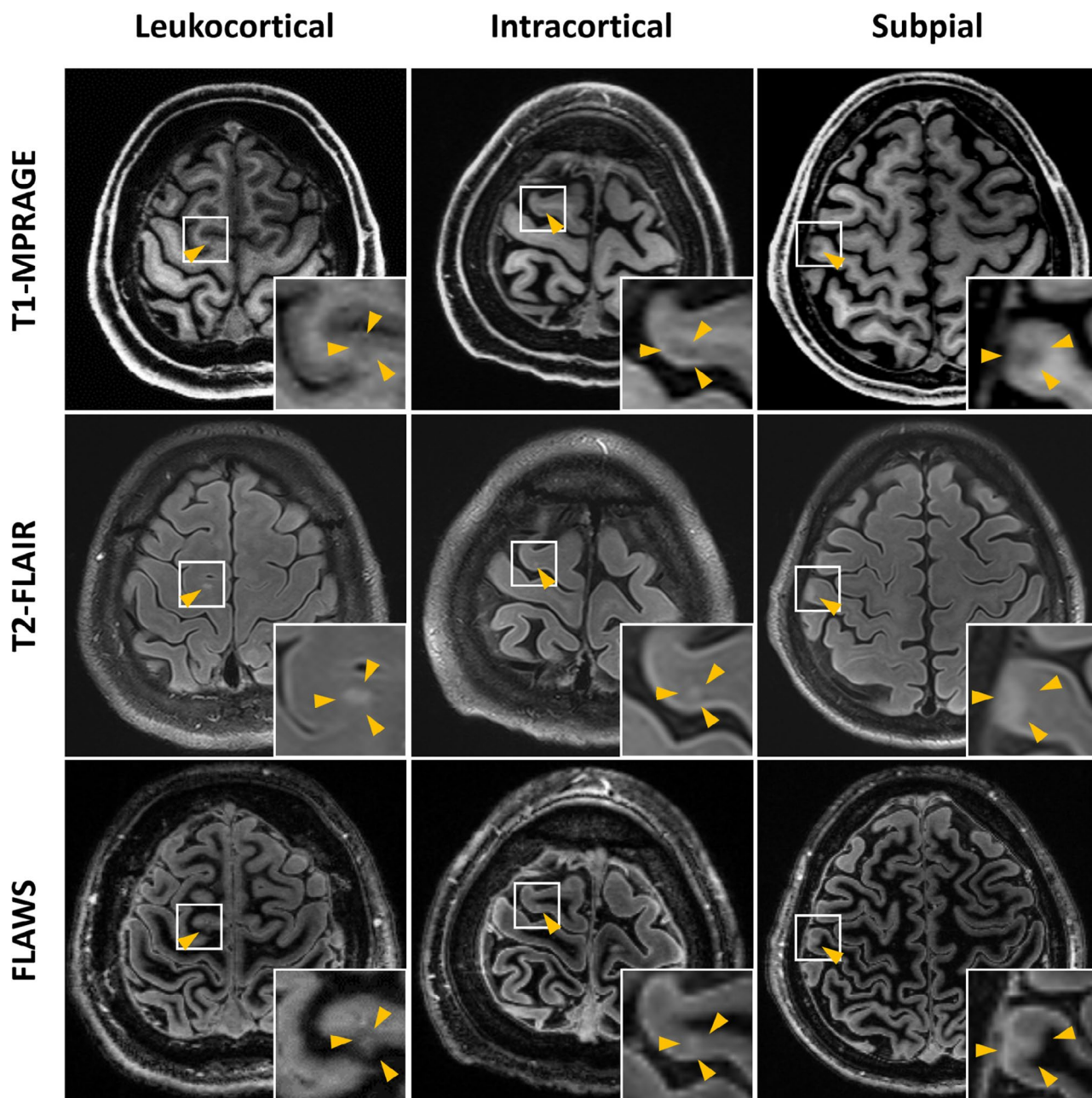
FIGURE 2 | Classification of cortical lesions with MOGAD under 7 T MRI. This figure shows three different types of cortical lesions in MOGAD patients obtained from T1-MPRAGE, T2-FLAIR, and FLAWS MRI. Lesions are highlighted by arrowhead. The top row shows lesions on T1-MPRAGE MRI. The middle row illustrates the same lesion on T2-FLAIR MRI. The bottom row illustrates the same lesion on FLAWS MRI. Three lesion subtypes were identified: Leukocortical lesions in the right frontal lobe, which involve the gray matter as well as the adjacent white matter at the gray/white matter junction. Intracortical lesion in the right frontal lobe. Subpial cortical lesion in the right frontal lobe.

the acute phase (12% vs. 0%, $p = 0.02$). Patients acquired in the German center also had a higher percentage of nodular paramagnetic lesions (25% vs. 9%, $p = 0.046$). A considerable proportion of MOGAD patients (243/282, 86%) did not exhibit lesions with SWI phase shift. No lesions presented diamagnetic phase changes (Table 2 and Table S5).

4 | Discussion

This is the first report on characterization of brain lesions in a cohort of MOGAD patients using 7 T MRI. Three types of

cortical lesions were identified in MOGAD, including subpial, intracortical, and leukocortical demyelination, with intracortical lesions being the most common. Both the number and proportion of lesions with MVS were higher than those with CVS. Furthermore, paramagnetic lesional phase shifts were rare and showed nodular changes and irregular borders in appearance.

Cortical demyelination is typical of MOGAD. Three lesion subtypes were identified in our study, with the highest proportion (16/31, 52%) being intracortical lesions; 31 cortical lesions were identified in 12 patients of 45 MOGAD patients. This finding confirms previous pathological studies [7, 8] that
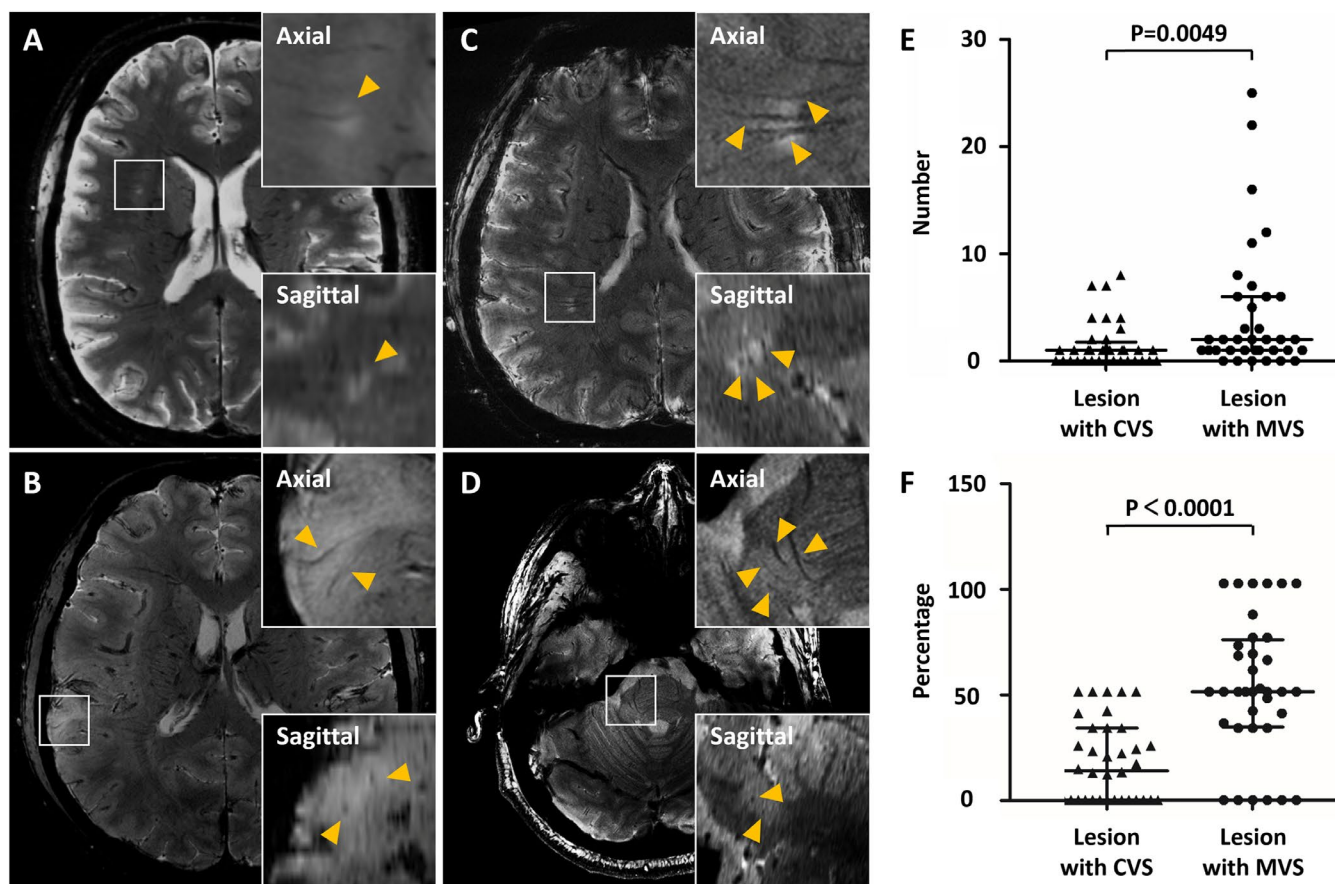
FIGURE 3 | Central vein sign and multiple veins sign of MOGAD lesions on 7T MRI. This figure illustrates exemplary CVS of white matter (A) and MVS of cortex (B), white matter (C), and brainstem (D) observed in MOGAD lesions on T2* weighted MRI. Veins were displayed in two perpendicular planes as a thin hypointense line or small hypointense dot (arrowheads). The figure also shows the comparison of the number (E) and percentage (F) between CVS and MVS. CVS, central vein sign; MVS, multiple veins sign.

showed cortical demyelinating lesions in postmortem brain slices of MOGAD, including subpial, intracortical, and leukocortical demyelination, and the ratio of intracortical lesions to be the highest among lesion types [7]. A recent 3 T MRI-based study [18] of cortical lesions in MOGAD showed only one intracortical lesion in one MOGAD patient but no other types of cortical lesions, which may be explained by the limited spatial resolution of 3 T MRI to detect cortical lesions in vivo and may also be related to the cohort of patients without focal cortical encephalitis. A previous study [3] regarding patients with seizures in MOGAD did report FLAMES to be associated with cortical lesions in MOGAD. Our cohort also exhibited this imaging feature, with MRI images showing unilateral cortical T2-FLAIR diffuse hyperintense signal alteration that did not involve the adjacent juxtacortical white matter. Although we found cortical lesions in nearly a quarter of MOGAD patients (12/45), 58% (7/12) had no clinical demyelination events with cerebral cortical encephalitis, which may indicate that other cortical symptoms, such as physical disability and cognitive impairment, may need to be evaluated more comprehensively in future studies.

Of interest, CVS was found in 19% of MOGAD lesions in our 7T MRI study. CVS has just been recognized in previous 1.5 and 3 T MRI examinations in MOGAD, with widely varying results. One study [18] showed that CVS was found in 78% (21/27) of MOGAD lesions, while another study [14] found that CVS was only found in 14.1% of all MOGAD lesions. The differing findings from the aforementioned studies may be related to the difference in the types of clinical demyelination events and MRI spatial resolution. There were both lesions containing one vein and lesions containing multiple veins in our cohort. This is consistent with the reported pathological findings, which had both perivenous and large white matter demyelination [7, 8, 19]. Our study found 19% of MOGAD lesions with CVS and 55% lesions with MVS. The number and percentage of MVS lesions found for each patient were higher than those of CVS lesions in our MOGAD patients. The lesions of MOGAD had perivenous inflammation, but the majority of lesions contained multiple veins, which may be one of the characteristics that distinguish MOGAD from other CNS demyelinating diseases. Although previous studies on CVS have focused on white matter lesions, CVS was also found in cortical and infratentorial lesions in our study, likely due to the enhanced spatial resolution and magnetic susceptibility of 7 T. The value of CVS in distinguishing MOGAD and MS should be further explored based on 7 T MRI.

In the present study, there were 39 (39/282, 14%) lesions with paramagnetic phase changes in eight MOGAD patients (8/45, 18%), showing nodular alterations and irregular borders in appearance. Of note, we observed that the presence of nodular
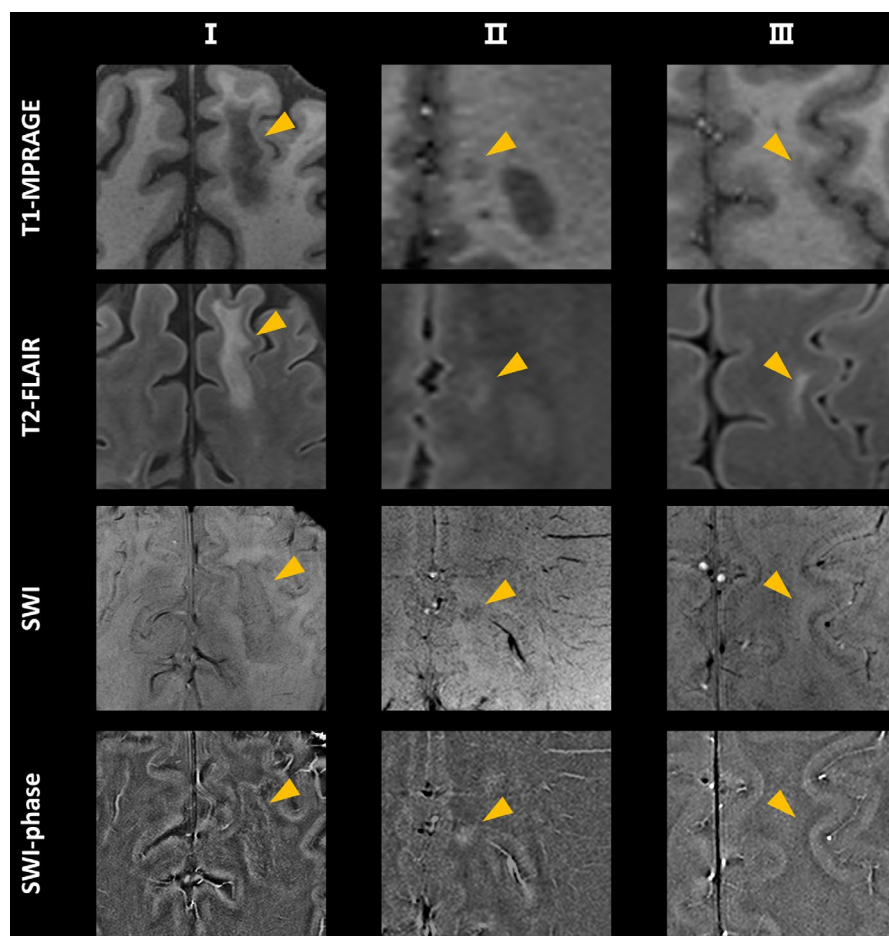
FIGURE 4 | Lesion characteristics on SWI in MOGAD patients under 7T MRI. This figure shows three different types of morphological and phase changes of MOGAD lesions obtained from T1-MPRAGE, T2-FLAIR, SWI, and SWI-phase MRI. Lesions are marked by arrowheads. The top row shows lesions on T1-MPRAGE MRI. The other rows demonstrate the same lesion on T2-FLAIR, SWI, and SWI-phase MRI, respectively. Three lesion subtypes were identified; Type I: A subcortical white matter lesion with paramagnetic irregular border and hypointense signal on SWI. Type II: A white matter lesion with paramagnetic nodule and hypointense signal on SWI. Type III: A juxtacortical white matter lesion without phase changes and isointense signals on SWI.

paramagnetic lesions was significantly higher in patients in the non-acute phase of MOGAD, while other clinical and MRI characteristics, including cortical lesion frequency, did not differ significantly between the acute and non-acute phases. While paramagnetic rim lesions are considered to represent chronic activity in multiple sclerosis [20], the origin and potential clinical significance of nodular paramagnetic lesions in MOGAD remain elusive. However, our findings underline the importance of the timing of MRI acquisition in future studies investigating lesion evaluation and its relationship with clinical disease burden in MOGAD patients. Previous studies on the paramagnetic phase shifts indicate that its pathological origin lies in the weakening of diamagnetism and the enhancement of paramagnetism caused by the destruction of brain structure [21]. The latter's damage includes demyelination and oxidative stress caused by iron deposition. Iron deposition may originate from the myelin sheath of oligodendrocytes engulfed by microglia and macrophages [10, 22], and may also stem from the deposition of ferritin and hemosiderin [22–24]. MOG-dominant myelin loss and perivascular MOG-laden macrophages were observed in recent pathological studies of MOGAD [7, 8], which indicates that

lesions with paramagnetic phase shifts in MOGAD patients may be caused by the loss of myelin and iron deposition. However, the pathophysiological mechanisms of phase shift and distinct lesion morphology still remain unclear. In the future, MRI and PET investigations should be combined to explore the behavior of inflammatory cells at the lesion sites with paramagnetic phase changes, and longitudinal studies are needed to explore the evolution of these lesions.

There are some limitations to our study. Firstly, our study has a cross-sectional design with a relatively small sample size. However, due to the relatively low incidence of MOGAD in the population and the restrictive exclusion criteria for 7T MRI, we believe this sample size is rather large for a 7T study of MOGAD. Secondly, the phenotype of spinal cord lesions in MOGAD was not studied. The lack of a concomitant comparator group of NMOSD or MS patients is a recognized limitation of our study. Our findings also revealed differences in a subset of clinical and MRI characteristics of MOGAD patients from different centers, which suggests geographic and ethnic factors to have an impact on disease manifestations, imaging features, and outcomes

across populations [25], highlighting the need for future diagnostic and treatment studies in diverse patient groups.

In this international two-center study, we found three different types of cortical lesions, with intracortical lesions being the most common. Although CVS lesions were also seen in MOGAD patients, the lesions with MVS were more common. Furthermore, lesions with paramagnetic phase changes are rare, and all were non-rim-like in appearance. These imaging features of brain lesions in MOGAD are clearly recognized by 7 T MRI and provide new insights into MOGAD.

Conflicts of Interest

The authors declare no conflicts of interest.

Data Availability Statement

The de-identified data from patients from Beijing Tiantan Hospital will be available for investigators following approval from the Institutional Review Board of Beijing Tiantan Hospital (Beijing, China).

References

1. B. Banwell, J. L. Bennett, R. Marignier, et al., "Diagnosis of Myelin Oligodendrocyte Glycoprotein Antibody-Associated Disease: International MOGAD Panel Proposed Criteria," *Lancet Neurology* 22 (2023): 268–282.

2. E. Sechi, L. Cacciaguerra, J. J. Chen, et al., "Myelin Oligodendrocyte Glycoprotein Antibody-Associated Disease (MOGAD): A Review of Clinical and MRI Features, Diagnosis, and Management," *Frontiers in Neurology* 13 (2022): 885218.

3. R. Ogawa, I. Nakashima, T. Takahashi, et al., "MOG Antibody-Positive, Benign, Unilateral, Cerebral Cortical Encephalitis With Epilepsy," *Neurology Neuroimmunology & Neuroinflammation* 4 (2017): e322.

4. D. Tzanetakos, J. S. Tzartos, A. G. Vakrakou, et al., "Cortical Involvement and Leptomeningeal Inflammation in Myelin Oligodendrocyte Glycoprotein Antibody Disease: A Three-Dimensional Fluid-Attenuated Inversion Recovery MRI Study," *Multiple Sclerosis* 28 (2022): 718–729.

5. D. Dubey, S. J. Pittock, K. N. Krecke, et al., "Clinical, Radiologic, and Prognostic Features of Myelitis Associated With Myelin Oligodendrocyte Glycoprotein Autoantibody," *JAMA Neurology* 76 (2019): 301–309.

6. S. A. Banks, P. P. Morris, J. J. Chen, et al., "Brainstem and Cerebellar Involvement in MOG-IgG-Associated Disorder Versus Aquaporin-4-IgG and MS," *Journal of Neurology, Neurosurgery, and Psychiatry* 92 (2020): 384–390, https://doi.org/10.1136/jnnp-2020-325121.

7. R. Höftberger, Y. Guo, E. P. Flanagan, et al., "The Pathology of Central Nervous System Inflammatory Demyelinating Disease Accompanying Myelin Oligodendrocyte Glycoprotein Autoantibody," *Acta Neuropathologica* 139 (2020): 875–892.

8. Y. Takai, T. Misu, K. Kaneko, et al., "Myelin Oligodendrocyte Glycoprotein Antibody-Associated Disease: An Immunopathological Study," *Brain* 143 (2020): 1431–1446.

9. P. Sati, J. Oh, R. T. Constable, et al., "The Central Vein Sign and Its Clinical Evaluation for the Diagnosis of Multiple Sclerosis: A Consensus Statement From the North American Imaging in Multiple Sclerosis Cooperative," *Nature Reviews Neurology* 12, no. 12 (2016): 714–722.

10. M. Absinta, D. Maric, M. Gharagozloo, et al., "A Lymphocyte-Microglia-Astrocyte Axis in Chronic Active Multiple Sclerosis," *Nature* 597 (2021): 709–714.

11. S. Trattnig, E. Springer, W. Bogner, et al., "Key Clinical Benefits of Neuroimaging at 7T," *NeuroImage* 168 (2018): 477–489.

12. T. Sinnecker, J. Kuchling, P. Dusek, et al., "Ultrahigh Field MRI in Clinical Neuroimmunology: A Potential Contribution to Improved Diagnostics and Personalised Disease Management," *EPMA Journal* 6 (2015): 16.

13. J. Kuchling, C. Ramien, I. Bozin, et al., "Identical Lesion Morphology in Primary Progressive and Relapsing-Remitting MS: An Ultrahigh Field MRI Study," *Multiple Sclerosis Journal* 20, no. 14 (2014): 1866–1871.

14. J. R. Ciotti, N. S. Eby, M. R. Brier, et al., "Central Vein Sign and Other Radiographic Features Distinguishing Myelin Oligodendrocyte Glycoprotein Antibody Disease From Multiple Sclerosis and Aquaporin-4 Antibody-Positive Neuromyelitis Optica," *Multiple Sclerosis* 28 (2022): 49–60.

15. D. M. Harrison, S. Roy, J. Oh, et al., "Association of Cortical Lesion Burden on 7-T Magnetic Resonance Imaging With Cognition and Disability in Multiple Sclerosis," *JAMA Neurology* 72 (2015): 1004–1012.

16. J. W. Peterson, L. Bö, S. Mörk, A. Chang, and B. D. Trapp, "Transected Neurites, Apoptotic Neurons, and Reduced Inflammation in Cortical Multiple Sclerosis Lesions," *Annals of Neurology* 50 (2001): 389–400.

17. T. Sinnecker, S. Schumacher, K. Mueller, et al., "MRI Phase Changes in Multiple Sclerosis vs Neuromyelitis Optica Lesions at 7T," *Neurology Neuroimmunology & Neuroinflammation* 3 (2016): e259.

18. R. Cortese, F. Prados Carrasco, C. Tur, et al., "Differentiating Multiple Sclerosis From AQP4-Neuromyelitis Optica Spectrum Disorder and MOG-Antibody Disease With Imaging," *Neurology* 100 (2023): e308–e323.

19. M. S. Weber, T. Derfuss, I. Metz, and W. Brück, "Defining Distinct Features of Anti-MOG Antibody Associated Central Nervous System Demyelination," *Therapeutic Advances in Neurological Disorders* 11 (2018): 1756286418762083.

20. F. Bagnato, P. Sati, C. C. Hemond, et al., "Imaging Chronic Active Lesions in Multiple Sclerosis: A Consensus Statement," *Brain* 147 (2024): 2913–2933.

21. Y. Zhang, S. A. Gauthier, A. Gupta, et al., "Quantitative Susceptibility Mapping and R2* Measured Changes During White Matter Lesion Development in Multiple Sclerosis: Myelin Breakdown, Myelin Debris Degradation and Removal, and Iron Accumulation," *AJNR. American Journal of Neuroradiology* 37 (2016): 1629–1635.

22. F. Bagnato, S. Hametner, B. Yao, et al., "Tracking Iron in Multiple Sclerosis: A Combined Imaging and Histopathological Study at 7 Tesla," *Brain* 134 (2011): 3602–3615.

23. S. Hametner, I. Wimmer, L. Haider, S. Pfeifenbring, W. Brück, and H. Lassmann, "Iron and Neurodegeneration in the Multiple Sclerosis Brain," *Annals of Neurology* 74 (2013): 848–861.

24. B. F. Popescu, J. M. Frischer, S. M. Webb, et al., "Pathogenic Implications of Distinct Patterns of Iron and Zinc in Chronic MS Lesions," *Acta Neuropathologica* 134 (2017): 45–64.

25. Z. M. Ong, M. Arip, Y. M. Ching, et al., "The Prevalence, Demographics, Clinical Features, Neuroimaging, and Inter-Ethnic Differences of MOGAD in Malaysia With Global Perspectives," *Multiple Sclerosis and Related Disorders* 67 (2022): 104168.

Supporting Information

Additional supporting information can be found online in the Supporting Information section.